

## Occurrence of Glass Transitions in Long-Chain Phosphatidylcholine Mesophases

Evgeniy Y. Shalaev,<sup>\*,†</sup> George Zografi,<sup>‡</sup> and Peter L. Steponkus<sup>§</sup>*Groton Laboratories, Pfizer Inc., Groton, Connecticut 06340, and School of Pharmacy, University of Wisconsin-Madison, Madison, Wisconsin 53705**Received: October 29, 2009; Revised Manuscript Received: February 2, 2010*

Several phosphatidylcholine (PC) species were studied by differential scanning calorimetry at different levels of hydration. A glass transition was observed in both lamellar gel and nonlamellar phases, with the glass transition temperature,  $T_g$ , decreasing as water content was increased. The structure of the lipid mesophase has a major impact on  $T_g$ , with the lamellar gel phase having a higher  $T_g$  than that of nonlamellar phases of the same lipid. While the headgroup has a noticeable influence on the  $T_g$ , changing the chain length, on the other hand, has less of an impact. The values of the calorimetric  $T_g$  were compared with other measures of molecular mobility in the PC species at comparable water contents reported in the literature. Observation of a  $T_g$  in different phosphatidylethanolamines (PE), as previously reported, and PC species in this study suggests that a glass transition can be expected to be a common feature of biological membranes and phospholipid bilayer preparations, such as liposomes.

## Introduction

Phospholipid preparations have often been used as model systems to study various structural features of biological membranes, as well as related physiological functions.<sup>1,2</sup> For example, investigations of the responses of biological membranes and other biological systems to stresses caused by dehydration and freezing have commonly involved using such model phospholipid systems.<sup>3</sup> Many structural and dynamic properties of phospholipids are interrelated and depend on the particular phase state, e.g., lamellar liquid crystalline vs gel. In turn, the occurrence of such phase behavior is strongly dependent on the temperature and level of hydration. For example, both cooling and dehydration of the lamellar liquid crystalline phase promote the liquid-crystal-to-gel phase transition, with a corresponding sharply decreased molecular motion in the bilayer.<sup>4</sup> In the absence of such structural phase changes, cooling and dehydration in a particular phase still can result in an abrupt slowing of molecular motion as reflected in an increase in the relaxation time. This reduction in molecular mobility of phospholipids appears to be associated with a glass transition, which occurs over a relatively narrow temperature range.<sup>5</sup> Glass transitions, i.e., transformations of a material with dynamic disorder to a state in which the disorder is “frozen” on an experimental time scale are commonly observed with a wide range of materials, e.g., metals, inorganic oxides, polymers, and carbohydrates. A typical glass transition in such systems is characterized by a relaxation time of about 200 s<sup>6</sup> and a length scale of several nanometers.<sup>7</sup> Glass transitions also have been shown to occur in certain types of thermotropic crystal mesophases, such as liquid crystals and plastic crystals.<sup>8</sup> Since many phases observed in phospholipid systems can be characterized as crystal mesophases, it is to be expected that under certain conditions they would exhibit glass transitions.

It is well established that physical and chemical stability of glass formers, in general, will improve significantly as the temperature is decreased below the glass transition temperature,  $T_g$ .<sup>9</sup> For example, amorphous-to-crystalline transitions can be prevented as the temperature is brought below  $T_g$  in many systems.<sup>10</sup> Similarly, the rate of chemical reactivity of molecules in the amorphous solid state significantly decreases below  $T_g$ .<sup>11</sup> Also, the so-called “dynamic” transition in folded proteins, which is believed to be equivalent to a glass transition,<sup>12</sup> has been shown to be associated with major changes in the rates of different biological processes, e.g., for the bacteriorhodopsin photocycle.<sup>13</sup> Overall, the formation of the glassy state, and the corresponding significant reduction in molecular mobility, would be expected to be associated with superior long-term stability in a variety of systems, including biological membranes, proteins, and small molecular weight pharmaceuticals.<sup>9,14,15</sup> For example, the stabilizing properties of sugars, which are known to protect proteins, liposomes, cells, and other biological systems against freezing and desiccation, are often related to the formation of a rigid glassy state by an amorphous sugar matrix.<sup>16–18</sup>

While there have been many studies of the glass transition in sugars, proteins, and synthetic polymers, there are only a few reports of experimental<sup>19–21</sup> and theoretical<sup>22,23</sup> studies on the appearance of a glass transition in membrane-related systems, such as lipid mixtures<sup>19,20</sup> and purple membranes.<sup>21</sup> Previous studies by Shalaev and Steponkus in model phosphatidylethanolamine (PE) systems reported, for the first time,<sup>5,24</sup> the observation of a glass transition with synthetic phospholipids. The  $T_g$  of these phospholipids had properties that were typically expected for other disordered systems, e.g., nonexponential relaxation behavior and plasticization by water. The molecular origin of the  $T_g$  in phospholipids, however, was suggested to be different from that observed in common amorphous materials, where the glass transition is generally associated with cooperative translational and rotational molecular motion. For PE species, which form partially ordered structures, the glass transition is likely associated with rotational rearrangements of either the entire phospholipid molecule or of only the headgroups or lipid chains. Note that, while a glass transition was observed

\* Corresponding author. E-mail: evgeniy.y.shalaev@pfizer.com.

<sup>†</sup> Pfizer Inc.

<sup>‡</sup> University of Wisconsin-Madison.

<sup>§</sup> Deceased. Past address: Department of Crop and Soil Sciences, Cornell University, Ithaca, NY 14853.

in several PE species, there have been no systematic studies of the  $T_g$  in another major class of membrane phospholipids, the phosphatidylcholines (PC). In the current study, we have investigated  $T_g$  in a series of long-chain phosphatidylcholines differing in the structure of their acyl chains. First, we attempted to explore the impact of the headgroup on the  $T_g$  through the use of 1,2-dioleoyl-*sn*-glycero-3-phosphocholine (DOPC), and to compare it with data for 1,2-dioleoyl-*sn*-glycero-3-phosphatidylethanolamine (DOPE) reported elsewhere.<sup>24</sup> Then we wanted to observe the  $T_g$  in the widely studied phospholipid, 1,2-dipalmitoyl-*sn*-glycero-3-phosphocholine (DPPC). To investigate the effect of acyl chain length on  $T_g$ , we compared DPPC to another saturated PC species, 1,2-dimyristoyl-*sn*-glycerol-3-phosphocholine (DMPC). Finally, plasticization of the  $T_g$  in various PC species by sorbed water was studied.

## Materials and Methods

**Preparation of Partially Hydrated Phospholipids.** 1,2-Dipalmitoyl-*sn*-glycero-3-phosphocholine (DPPC, 16:0), 1,2-dioleoyl-*sn*-glycero-3-phosphocholine (DOPC, 18:1 *cis*), and 1,2-dimyristoyl-*sn*-glycerol-3-phosphocholine (DMPC, 14:0) were purchased from Avanti Polar Lipids as a chloroform solution and used without further purification. Chloroform was removed under a stream of  $N_2$  at room temperature, followed by drying under vacuum conditions for at least 15 h. Liposomes were prepared in double-distilled, deionized, water, saturated with  $N_2$ , by freeze–thaw cycling between liquid nitrogen and a water bath, with vortexing between cycles; ten freeze–thaw cycles were employed. The temperature of the water bath was chosen to be slightly above the chain-melting temperature for each phospholipid. The lipid concentration generally ranged from 100 to 200 mg lipid/mL water.

Partially hydrated phospholipids for DSC experiments were prepared in DSC pans through equilibration with water vapor at various relative humidities (RH). Saturated aqueous solutions of KCl, NaCl, NaBr,  $MgCl_2$ , and LiCl were used to maintain RH values of 84, 75, 56, 32%, and 11%, respectively. DSC pans containing either fully hydrated liposomes or dried lipids, approximately 1–2 mg (dry weight) of lipid per pan, were placed over saturated salt solutions in tightly closed jars, or in desiccators to expose samples to a particular RH. The jars were flushed with argon, whereas the desiccators were evacuated with a vacuum pump, and the mixtures were equilibrated for 7–9 days. The equilibration temperature was maintained at 30 °C in a low-temperature incubator, VWR Scientific, Model 2005. After equilibration, the DSC pans were sealed hermetically.

**DSC Experiments.** DSC experiments were performed with a Perkin-Elmer DSC-7 instrument and hermetically sealed aluminum pans. An empty aluminum pan was used as a reference. The instrument was calibrated using the melting points of water and indium. Two types of thermal programs were used in DSC experiments. In the majority of experiments, samples were cooled to  $\leq -120$  °C, followed by immediate rapid heating to  $\geq 30$  °C; such cooling–heating cycles were repeated several times. In the annealing experiments, samples were cooled to  $-140$  °C, then immediately heated to the specified annealing temperature, followed by holding the samples at the annealing temperature for different periods of time, cooling to  $-100$  to  $-140$  °C, and finally heating to above the  $T_g$ . After each annealing scan, the regular cooling–heating scan was repeated to obtain results for a sample with an erased thermal history. Heating and cooling rates generally were maintained at 40 °C/min; at such a high heating rate the apparent melting temperatures of water and indium were 0.7–1.5 °C higher than those

obtained at a scanning rate of 10 °C/min. This temperature difference was not considered significant for the purposes of this study, and, therefore, we did not try to correct the transition temperatures obtained at the higher scanning rate. All DSC pans were weighed before and after an experiment to confirm that the water content did not change during the experiment. After DSC runs, the water content was measured in all of the samples (see below). The glass transition temperatures, reported in this study, were determined as onset temperatures.

**Water Content Determination.** The water contents of all individual DSC samples were determined gravimetrically, after DSC experiments, by drying phospholipids in DSC pans with pin holes at 70 °C in a vacuum until a constant weight was achieved (usually 3.5 h), as described in ref 25. Water content values obtained after equilibration of both liposomes and dried lipids at different RH conditions, as well as the temperatures of DSC thermal events, are summarized in the Supporting Information.

## Results

**DOPC–Water System.** Representative DSC heating curves for partially dehydrated DOPC samples are shown in Figure 1. A main endothermic peak, representing the  $L_\beta$ -to- $L_\alpha$  phase transition,  $T_m$ , was observed for the samples equilibrated at 32–84% RH. Water did not crystallize in any of the samples under the condition of these experiments. The values of  $T_m$  increased with increasing dehydration as expected. The DSC curves for samples that were partially hydrated from the dried state at the same RH levels as given above, and all had a similar appearance and transition temperatures to that prepared by dehydration (examples of DSC curves for both hydrated and dehydrated DOPC samples, as well as the transition temperatures are given in the Supporting Information). The DSC curves for the “dry” DOPC sample, i.e., a water content of approximately 1 wt %, contained no major thermal events that could be associated with the main transition temperature,  $T_m$ . This likely indicates that this preparation exists in a nonlamellar phase, which is consistent with the phase diagram of the DOPC–water system reported in.<sup>26</sup> Note also that a weak endotherm, with an enthalpy change more than one order of magnitude lower than that expected for  $T_m$ , was observed at approximately 60 °C. This event is likely associated with a transformation between two nonlamellar phases, probably between cubic and inverted hexagonal phases.<sup>26</sup>

In addition to the  $T_m$  peak, relatively weak thermal events were observed at lower temperatures, as shown in Figure 1B. The shape of this transition, i.e., the endothermic nature and stepwise change in the heat flow, closely resemble what is generally observed with the glass transition commonly detected in different disordered states, including amorphous and liquid crystalline materials. To ascertain whether any relationship to a glass transition exists, annealing experiments were performed. Examples of DSC curves obtained after annealing these samples at temperatures slightly below the transitions of interest, marked as  $T_g$ , are shown in Figure 1B as broken lines. In the annealed samples, endothermic peaks, reflecting enthalpy recovery after enthalpy relaxation, were observed after annealing; the extent of relaxation increased with increasing time allowed for annealing to occur. Since such behavior is commonly observed after annealing amorphous materials below the glass transition temperature, we conclude that this event is the glass transition of the gel phase for these partially hydrated phospholipid samples.

The DSC curves for the “dry” DOPC (water content 1%, nonlamellar, possibly cubic,<sup>26</sup> phase), on the other hand, had

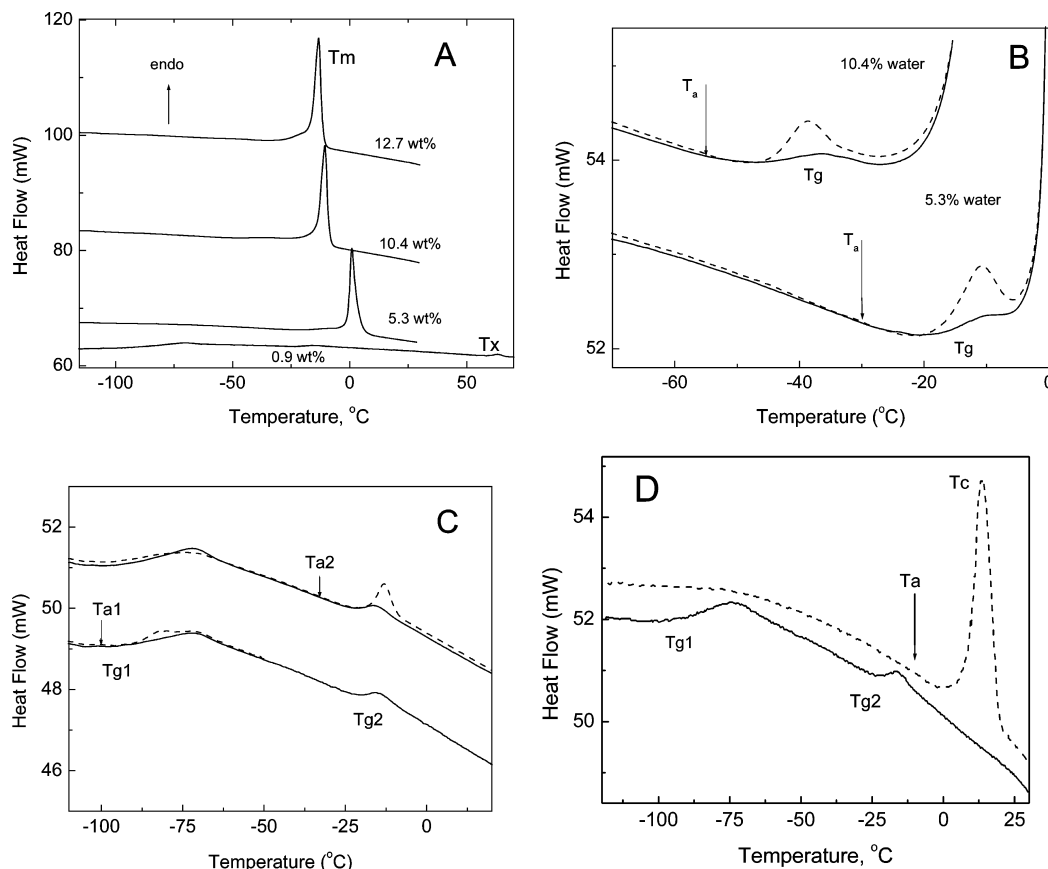


**Figure 1.** Representative DSC heating curves of DOPC. (A) Samples were dehydrated from fully hydrated liposomes at 84, 75, and 32% RH (top three curves); the bottom curve is for the initial dried lipid (prior to liposome preparation). Numbers show residual water content for particular DSC samples. DSC curves in this and other figures are shifted vertically. (B) Magnified low-temperature part of DSC curves of DOPC with 10.4 and 5.3 wt % water. Dashed lines, after annealing; solid lines, after heating above the  $T_g$ . Annealing was performed at  $T_a = -30$  °C for 64 min (5.3% water) and at  $T_a = -55$  °C for 60 min (10.4% water). (C) DSC curves of dried sample (1.0 wt % water). Dashed lines, after annealing for 60 min at temperatures  $T_{a1} = -100$  °C and  $T_{a2} = -33$  °C; solid lines, after heating above the  $T_g$ . (D) DSC curves of dried DOPC showing impact of annealing above the  $T_{g2}$ . Dashed line: after annealing at  $T_a = -10$  °C for 63 min.

two endothermic steps at approximately  $-95$  and  $-20$  °C that also resemble a thermal event arising from the presence of a  $T_g$  (Figure 1C). Annealing below the  $T_g$  events, indeed, resulted in enthalpy recovery endotherms. Therefore, both thermal events represent glass transitions. The existence of two  $T_g$  events may be indicative of the coexistence of two phases with different glass transition temperatures, as is commonly observed in polymers and other disordered materials. The higher  $T_g$  can be attributed to the  $T_g$  of DOPC in a nonlamellar (cubic) phase whereas the origin of the lower  $T_g$  event is less certain. This suggestion will be considered further in some detail in the Discussion section.

When the “dry” DOPC sample was annealed at  $-10$  °C (i.e., above the event marked as  $T_{g2}$  in Figure 1C), a different thermal behavior was observed (Figure 1D).  $T_g$  events were no longer detected, whereas a strong endothermic peak was observed on the first heating scan. On the second heating scan, the endothermic peak was not observed, whereas the two  $T_g$ s were detected again (Figure 1D, solid curve). The appearance of such irreversible thermal behavior is typical for the presence of a lamellar crystalline,  $L_c$ , phase, with the three-dimensional order of a crystal.<sup>27</sup> These results, therefore, suggest that the annealing of phospholipids above  $T_g$  can promote the formation of a more ordered state whereas keeping samples below the  $T_g$  may prevent the phase transition from occurring. It is well-known for many organic glass-formers that crystallization is usually observed above the  $T_g$  whereas storage below  $T_g$  tends to prevent crystallization on a scale of months and years.

**DMPC–Water System.** DMPC samples exhibited more complex thermal behavior than DOPC, depending on the relative humidity and whether samples were prepared by dehydration or hydration. For DMPC samples dehydrated at both high (84 and 75%) and low (11%) RH values, DSC curves exhibited  $T_m$  (Figure 2A) and  $T_g$  (Figure 2B) events, that were similar to DOPC results, with the appearance of  $T_g$  being enhanced by annealing as described above. In addition, a weak endothermic peak, the so-called pretransition, was typically observed. The pretransition is generally assumed to be associated with the transformation from the gel ( $L_{\beta}'$ ) to ripple ( $P_{\beta}'$ ) phases.<sup>28</sup> In DMPC samples dehydrated at intermediate RH values (56 and 32%) and in all DMPC samples hydrated from the dried state at RH 32 to 84%, however, a different behavior was observed (Figure 2A, curves c and d). The first heating curves exhibited a strong endotherm without any evidence of the lower-temperature thermal events, whereas during second heating scans the  $T_g$  and relatively strong (but weaker than that on the first scan) endothermic  $T_m$  peak(s) were detected. As mentioned above, such a difference between the first and second DSC scans is typical for phospholipids in the lamellar crystalline state. In the DMPC case, the  $T_c$  event corresponds to the  $L_c$ -to- $L_{\alpha}$  transition during the first heating scan. When the DSC sample is cooled, crystallization, i.e., the  $L_{\alpha}$ -to- $L_c$  conversion, does not usually occur during the cooling scan. Instead, the  $L_{\alpha}$  phase converts into a metastable ripple or gel phase during cooling, resulting in appearance of  $T_m$  event during heating on the second DSC scan.

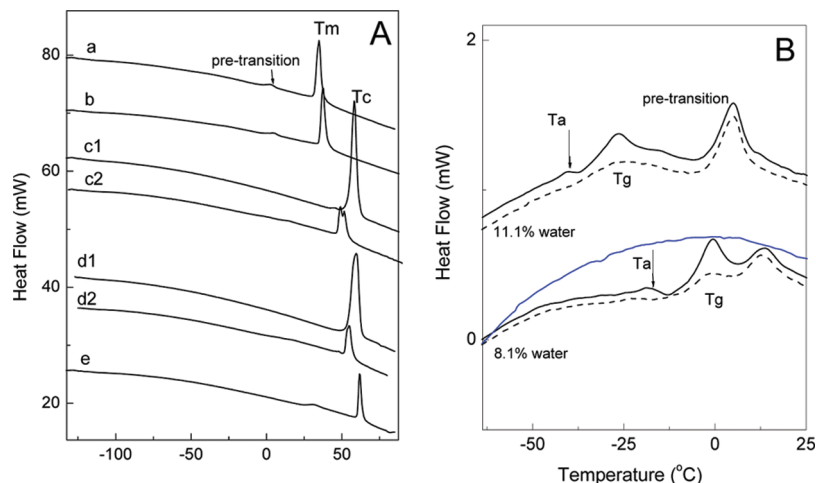


**Figure 2.** Representative DSC heating curves of DMPC samples dehydrated from fully hydrated liposomes. (A) Samples were equilibrated at different RH values as follows: (a) 84%, (b) 75%, (c) 56%, (d) 32%, (e) 11%. c1 and d1 represent first heating curves, whereas c2 and d2 represent second scans. (B) Magnified part of DSC heating curves of DMPC dehydrated at 75% RH (water content 11.1 wt %) and 56% (water content 8.1 wt %). Solid lines: after annealing at  $T_a = -40$  °C (11.1 wt % water) and  $T_a = -17$  °C (8.1 wt % water) for 30 min. Dashed lines: after heating above the  $T_g$  to eliminate thermal history. Blue line corresponds to c1 curve in Figure 2A demonstrating absence of  $T_g$  in the L<sub>c</sub> phase.

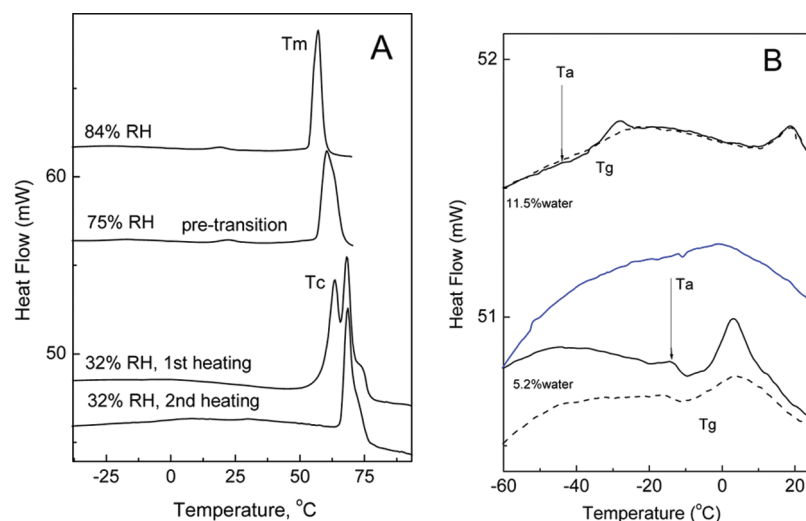


**Figure 3.** (A) Representative DSC heating curves of DPPC samples dehydrated at different RH from fully hydrated liposomes. (B) DSC heating curves of DPPC dehydrated at 84% RH (water content 11.5 wt %) and 32% RH (water content 5.2 wt %). Solid lines: after annealing at  $T_a = -44$  °C (11.5 wt % water) and  $T_a = -14$  °C (5.2 wt % water) for 30 min. Dashed lines: after heating above the  $T_g$  to eliminate thermal history. Blue line corresponds to "32% RH, 1st heating" curve in Figure 3A demonstrating an absence of  $T_g$  in the L<sub>c</sub> phase.

**DPPC–Water System.** Similar to DMPC, DPPC samples demonstrated two types of thermal behavior, with the apparently irreversible thermal behavior associated with the L<sub>c</sub> phase. Based on the DSC data, the L<sub>c</sub> phase occurred, either as the main phase or as one coexisting with the gel phase, in the samples dehydrated at 32% RH from the fully hydrated liposomes, and in the samples prepared by hydration of dehydrated lipid at 32 and 56% RH, as shown in Figure 3A using data for a sample equilibrated at 32% RH as an example. The  $T_g$  event was observed in the majority of DPPC samples, with exception of samples where L<sub>c</sub> was the dominant phase (Figure 3B). Overall, thermal behavior of DPPC samples closely resembled that of DMPC, i.e., another saturated lipid with a shorter (by two carbons) chain length.

## Discussion

**1. Major Factors That Influence Glass Transitions in Phospholipids.** The  $T_g$  values for three PC species in the gel phase are shown as a function of water content in Figure 4. In addition, the  $T_g$ s for DOPC in a nonlamellar (cubic) phase, as

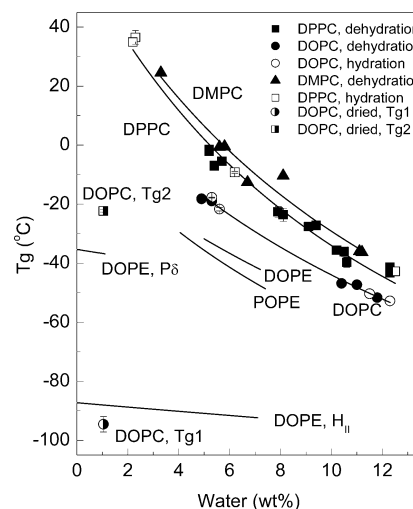


**Figure 4.** Glass transition temperatures for PC (this study) and PE<sup>5,24</sup> species as a function of water content. Lines are obtained by fitting experimental data to Gordon–Taylor equation.



**TABLE 1: Parameters of the Gordon–Taylor Equation for PC (This Study) and PE<sup>5,24</sup> Species**

lipid	phase	$T_{gL}$ ( $T_g$ of anhydrous lipid), K	$K$	water content, wt %
DPPC	$L_\beta$ or $L_\beta'$	$338.2 \pm 3.9$	$8.8 \pm 0.4$	5.2–12.3
DOPC	$L_\beta$	$296.4 \pm 2.1$	$6.4 \pm 0.2$	4.9–12.3
DMPC	$L_\beta$ or $L_\beta'$	$339.5 \pm 9.2$	$7.8 \pm 1.0$	3.3–11.2
DOPE	$L_\beta$	$259.6 \pm 9.8$	$3.5 \pm 1.5$	5.0–7.2
POPE	$L_\beta$	$277.2 \pm 10.4$	$7.3 \pm 1.7$	4.2–7.4
DOPE	$P_\delta$	$238.8 \pm 0.5$	$1.3 \pm 0.9$	0–1.1
DOPE	$H_{II}$	$185.9 \pm 1.3$	$1.4 \pm 0.8$	0–7.1 <sup>a</sup>

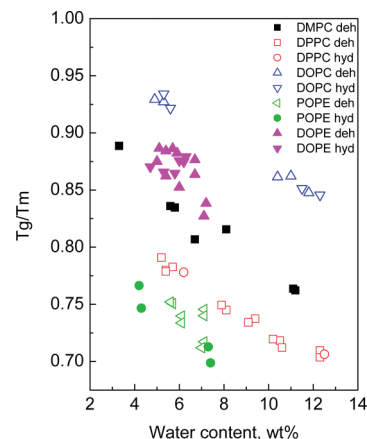
<sup>a</sup> Water content in the DOPE  $H_{II}$  phase was estimated with an assumption that DOPE hydration in the DOPE:sucrose mixtures is the same as DOPE alone dehydrated at the same osmotic pressure.

well as previously reported data for DOPE and POPE,<sup>5,24</sup> in different phases, are shown for comparison. The  $T_g$  decreased with an increase in water content, which is consistent with the plasticizing effect of water on the glass transition of other systems, e.g., sugars<sup>29</sup> and proteins.<sup>30</sup> To describe such plasticizing effects of water on the  $T_g$  of the phospholipids in terms of the individual components, the Gordon–Taylor (GT) equation has been used<sup>31</sup>

$$T_g = (w_1 T_{gL} + K w_2 T_{gw}) / (w_1 + K w_2) \quad (1)$$

where  $T_{gL}$  and  $T_{gw} = 134 \text{ K}$ <sup>32</sup> are the glass transition temperatures of the anhydrous phospholipid and water, respectively,  $w_1$  and  $w_2$  are the weight fractions of phospholipid and water, respectively, and  $K$  is a constant.

The experimental data are fitted to the GT equation with  $T_{gL}$  and  $K$  as fitting parameters. The fitted curves are shown in Figure 4 as solid lines.  $T_{gL}$  and  $K$  of the GT equation are given in Table 1. For the majority of the lipids studied,  $K$  values are 6.4–8.8, whereas lower values were obtained for DOPE. The lamellar gel phase of DOPE has a  $K$  value of 3.5, whereas the two nonlamellar phases possess even lower  $K$  values of 1.3 and 1.4 (Table 1). The  $K$  parameter in the GT equation can serve as a measure of the extent of plasticization, where a higher  $K$  value corresponds to stronger plasticization. Therefore, it would be interesting to compare the  $K$  values of phospholipids with another type of biological molecule containing water, i.e., sugars, which are known to protect biological membranes against freeze- and desiccation-induced damage. Sugars are reported to have  $K$  values between 3.7 and 7.8,<sup>33,34</sup> which are similar to the  $K$  values of PC and PE species in the lamellar gel phase. One may suggest that a similarity in the  $K$  values, combined with similar  $T_g$  in the dry state, would be a favorable factor in cryo- and lyoprotection of membranes by sugars. Indeed, such “coordinated”  $T_g$  changes upon freezing and/or desiccation would result in both sugar and membrane components entering the glassy state at the same time, thus minimizing mechanical strains. Otherwise, if there is a significant difference in the  $K$  and/or  $T_g$  values between a membrane and a would-be-cryoprotector matrix, the presence of one component in a glassy and another in a liquidlike (or rubbery) state would be expected to create significant mechanical strains due to differences in the thermal contraction coefficients between glassy (solid) and liquid states. Another important class of biological molecules, proteins, are generally plasticized by water to a lesser degree than sugars, with  $K$  values of 1.3–5 reported for protein–water systems.<sup>35</sup> Moreover, protein (e.g., myoglobin), when added to sugar systems, lowered  $K$  values by a factor of 2 or more, with  $K$  values of 1.9–3.3 reported for protein–sugar–water systems.<sup>34</sup> This observation opens an intriguing possibility that membrane proteins may reduce sensitivity of the membrane to

**Figure 5.**  $T_g/T_m$  (in kelvin) as a function of water content for PC and PE species.

water. Indeed, purple membrane preparations appeared to not be plasticized by water, with the  $T_g$  reported to be independent of hydration.<sup>21</sup> It should be noted as a word of caution, however, that the GT equation was theoretically derived based on an assumption of ideal volume additivity between two components of a mixture.<sup>31</sup> Whereas in the present work the GT equation is used as a convenient and empirical (from the perspective of this study) way to describe the plasticizing effects of water, and any fundamental significance of comparison of  $K$  values of lipids and cryo- and lyoprotectors, and protein and lipid components of biological membranes, remains to be explored.

Understanding the role of water on the various phase transitions observed with phospholipids is significant for understanding the mechanisms of freeze- and desiccation-induced damage of biological membranes and cells. It is of interest, therefore, to compare the impact of water on  $T_m$  and  $T_g$ . Both  $T_m$  and  $T_g$  increase with dehydration as expected; however, the impact of water on  $T_g$  is more pronounced than on  $T_m$ . To illustrate this difference, values of  $T_g/T_m$  are presented in Figure 5 as a function of water content for several PC and PE species in the gel phase. As can be seen,  $T_g/T_m$  increases with dehydration in a linear fashion, with a similar slope for the different lipids. The absolute  $T_g/T_m$  values, however, are different between lipid species, with no clear connections between  $T_g/T_m$  and the nature of the phospholipid.  $T_g/T_m$  varies between 0.7 (for POPE and DPPC at higher water contents) to above 0.9 (for DMPC at low water contents). Note that  $T_g/T_m \sim 0.7$  is a commonly reported value for many small organic molecules and polymer glass-formers, although some systems do exhibit values outside of this range.<sup>36</sup> Such representations may have some practical value as, for example, one can estimate  $T_g$  from known values of  $T_m$  recognizing that  $T_m$  data for phospholipids as a function of water content are widely available (e.g., ref 37), whereas  $T_g$  values are not.

While water content is a major factor influencing  $T_g$ , the phase state of a phospholipid has a significant impact as well.  $T_g$ , therefore, was measured for the same phospholipid in different phases, DOPC (this study) and DOPE.<sup>24</sup> In both lipids, the  $T_g$  was shown to be higher in the  $L_\beta$  phase (which has 2-dimensional translational order), than in the corresponding less ordered nonlamellar phase. For example, the  $T_g$  value for anhydrous DOPE in the  $L_\beta$  phase is 260 K (Table 1), followed by the ribbon phase ( $T_g = 239$  K) and the  $H_{II}$  phase ( $T_g = 186$  K). Similarly, the  $T_g$  value for the  $L_\beta$  phase of DOPC containing 1 wt % water is approximately 14 °C (extrapolated from results at higher water contents using the GT equation); this is significantly higher than a value of approximately -20 °C, measured for DOPC in the nonlamellar phase. The higher  $T_g$  of the  $L_\beta$  phase reflects a lower molecular mobility in this more ordered phase relative to the nonlamellar phases at comparable water content and temperature, as can be expected. Another significant (and potentially important) difference between the  $L_\beta$  and nonlamellar phases is the higher  $K$  value in the GT equation for the  $L_\beta$  phase of DOPE, 3.5 vs 1.3–1.4 for nonlamellar phases of the same lipid.

The headgroup is another significant factor which defines the  $T_g$  of phospholipids. In particular, comparing  $T_g$  data for DOPC (this study) and DOPE<sup>24</sup> (Figure 4), we propose that the PC species would be expected to have a higher  $T_g$  than a PE species with the same hydrocarbon tail at comparable water contents. In addition, the same trend of a higher  $T_g$  for PC species can be observed by comparing POPE (this study) vs POPC.<sup>38</sup> The  $T_g$  for POPC was reported to be approximately 260 K at a water content 10.6%,<sup>38</sup> compared to 211 K for POPE (obtained using the GT equation, Table 1). The length of the hydrocarbon tail, however, might have a lesser impact on the  $T_g$  of phospholipids than the factors considered above (i.e., water content, phase state, and headgroup). Indeed, an increase in the chain length from 14 to 16 had a minimal impact on the  $T_g$  of PC species (DPPC vs DMPC). Moreover, the  $K$  parameters of the GT equation for these two lipids are very similar (Table 1). Recognizing that the difference in the chain length between DPPC and DMPC is relatively small, we had attempted to extend the range of the chain length by using the 23:0 PC species (1,2-ditricosanoyl-*sn*-glycero-3-phosphocholine, DTPC, 23:0). Unfortunately, the DTPC results were inconclusive. While a weak endothermic event was detected in DTPC samples below the  $T_m$ , the enthalpy recovery (which was used as a “signature” of the glass transition) was not observed after annealing (DSC curves not shown). Therefore, considering the limited range of chain lengths that we studied, our suggestion that chain length likely is not a major factor for determining the  $T_g$  of phospholipids should be considered only as a preliminary consideration.

**2. Comparison of the Calorimetric  $T_g$  by DSC with Other Measures of Molecular Mobility.** It would be interesting to compare the DSC results reported in this study with other measures of molecular mobility performed with the same phospholipids in low-temperature/low-water content regions. In particular, three of the lipids used in this study, i.e., DPPC, DOPC, and DMPC, have been studied by neutron scattering,<sup>39</sup> anelastic spectroscopy,<sup>40</sup> and electron spin resonance (ESR),<sup>41</sup> respectively, as described below. The dynamics of DPPC with low water content (2–2.5%) have been studied by neutron scattering.<sup>39</sup> From the temperature dependence of the mean-square displacement of protons, three regimes were identified,<sup>39</sup> i.e., the vibrational regime (up to ~220 K), the localized regime (between 250 and 340 K), and the higher-temperature regime with translational motion associated with the gel-to-lamellar liquid crystalline transition (350–390 K). The calorimetric  $T_g$

for DPPC at a water content of 2% is ~300 K (this study), i.e., at the middle point of the “localized regime”. The localized regime, as defined by the neutron scattering, is characterized by a significant increase in rotational mobility, while translational mobility is absent. It should be noted that any direct comparison between neutron scattering and DSC is not straightforward because of a major difference in the experimental time scales, i.e.,  $10^{-9}$  s for neutron scattering vs  $10^2$  s for calorimetric  $T_g$ . In particular, the absence of translational motions in the localized regime on the neutron scatter (nanoseconds) time scale does not necessarily mean that such motions absent on the DSC time scale of 200 s.

In another study, several lipids and lipid mixtures, including DOPC, were examined by anelastic spectroscopy.<sup>40</sup> Although a water content, the sample preparation procedure, or the specific DOPC phase was not described, the study did mention that the water content in a sample containing lipid mixtures was approximately 3%. Therefore, we assume that samples studied in ref 40 represent dehydrated lipids and that it is reasonable to compare these results with the present study. The glass transition temperature was determined by anelastic spectroscopy to be 175 K and was suggested to be the glass transition of water molecules confined in the bilayer of DOPC.<sup>40</sup> Similarly, in the present study, a low-temperature glass transition event at -95 °C (178 K) was observed in dried DOPC by DSC. The likely origin of this event is discussed in some detail below.

Increased mobility of a probe molecule imbedded in the  $L_\beta'$  phase of DMPC (20% water) was observed by ESR measurements in the range of 50–210 K.<sup>41</sup> In the present study, the calorimetric  $T_g$  for DMPC at 20% water was determined to be 205 K (Table 1), which is within the “increased mobility” region of the spin label as described in ref 41. Interestingly, angular oscillations (librations) of the probe molecules were detected, whereas neither rotation along the long molecular axis nor small-scale translational mobility (around some “equilibrium” position) appeared to be significant.<sup>41</sup> Therefore, while the onset of local motions of the probe molecule appears to coincide with the  $T_g$  of the phospholipid matrix, rotation of the probe may remain “frozen” above the  $T_g$ . It is not obvious, however, if there are direct correlations between molecular motions of the spin label and those of the phospholipid molecules, and it is possible that phospholipid molecules may exhibit other types of molecular motions associated with the glass transition.

Overall, therefore, there appears to be reasonable agreement between the calorimetric  $T_g$  in this study and other measures of molecular mobility for the various PC species reported in the literature. The agreement between different methods indicates either that different methods are sensitive to the same type of molecular mobility, or (which is more likely) that there is a coupling between different molecular mobility modes. For example, note that neutron scattering also has been used to study dynamics in another important class of molecules, proteins, with a “dynamic transition” detected as a change in the temperature dependence of the mean square displacement. In the proteins, this dynamic transition was shown to occur in the same temperature range as the glass transition determined in several hydrated proteins by DSC, which is remarkable considering that different time scales are associated neutron scattering and DSC experiments.<sup>12</sup> A brief discussion of the molecular mobility as related to the  $T_g$  in phospholipids is given in the following section.

**3. Origin of the Glass Transition in Phospholipids.** The glass transition in small-molecular-weight amorphous solids is usually associated with the initiation (heating) or termination

(cooling) of cooperative long-scale translational motions, having a characteristic relaxation time of about 200 s. The translational mobility in these systems is usually coupled with rotational reorientations. In a different type of disordered materials, i.e., crystal mesophases such as plastic crystals and liquid crystals, rotational motion commences above the glass transition, whereas positional mobility remains “frozen”.<sup>42</sup> One could expect that phospholipids, which usually possess orientational and in many cases 1- and 2-dimensional positional order (as with the gel phase), would resemble crystal mesophases with rotational motion as the most likely source of the  $T_g$ .

Therefore, it is reasonable to suggest that the majority of the  $T_g$  events reported in this study arise from cooperative rotational motions of phospholipid molecules in the  $L_\beta$  phase, with such rotations being plasticized by water. This description leads to the next question—what type of rotational motion is related to the  $T_g$  observed in the lamellar gel phase, e.g., is it rotation of the entire molecule, its headgroup, or hydrocarbon tail? Several studies have addressed the question about possible mechanism of molecular mobility in the gel phase. In studies using dielectric spectroscopy and NMR, rotational mobility of the headgroups was detected well below  $T_m$ . For example, rotation of the headgroup, likely along the P–O bond, was observed in the  $L_\beta$  phase of DMPC by dielectric spectroscopy<sup>43</sup> at temperatures of 20 °C (14% water) to 40 °C (20% water) below  $T_m$ . Also, it was reported, based on NMR data, that rotational motion of phospholipid headgroups exists well below the  $T_m$  and is frozen only at much lower temperatures, below –40 °C.<sup>44</sup> In other studies, fast mobility modes of hydrocarbon tails were detected at low temperatures and low hydration levels. For example, in a study of DPPC at low water content (2–2.5%) by neutron scattering and atomistic simulations, substantial mobility of the hydrophobic tails was observed in the gel phase well below the  $T_m$ .<sup>39</sup> Also, dynamical transitions in DPPC, due to changes in the conformational state of hydrocarbon chains from the all-trans state of the chains to the excited state containing gauche configurations, were detected by Raman spectroscopy at ~200 K.<sup>45</sup> Therefore, although there are compelling arguments that the  $T_g$  in phospholipids is associated with a cooperative rotational motions, a question remains concerning what groups are involved in such  $T_g$ -associated rotations, i.e., headgroup or hydrocarbon tail.

Finally, it would be appropriate to address the topic of the  $T_g$  of water confined in a phospholipid mesophase. Indeed, one could expect that these water regions (e.g., interbilayer water in the lamellar phase) would exhibit the glass transition associated with amorphous water, in which case we should observe two separate  $T_g$  events (one for interbilayer water and one for the phospholipids). In this study, two  $T_g$  events were detected with DOPC in the cubic phase, and it seems reasonable to assume that the low-temperature  $T_g$  is related to the  $T_g$  of confined water, as was indeed suggested for DOPC based on anelastic spectroscopy.<sup>40</sup> It should be noted, however, that this DOPC sample had a low water content (1% w/w) and that it might be difficult to accept that such a low amount of water would result in a relatively strong DSC signal. Therefore, an alternative interpretation of the second  $T_g$  event in DOPC is that it is related to a second phospholipid phase, possibly the  $H_{II}$  phase coexisting with the cubic phase. In addition, in all other samples studied we observed only one  $T_g$  event. Obviously, water can influence and participate in motions of phospholipid molecules, and plasticization of the  $T_g$  by water is a clear example of such relationships. Also note that a dynamic coupling between mobility of the methyl group and the interbilayer water

molecules near the trimethylammonium group was reported.<sup>43</sup> Overall, we can conclude that in the present study we did not observe strong evidence for the  $T_g$  of water confined in phospholipid lamellar or nonlamellar phases, with the possible exception of DOPC in the cubic phase. We believe that the question of the  $T_g$  of water confined in phospholipid mesophase warrants further investigation.

## Conclusions

Glass transitions have been observed for PC and PE phospholipids in gel phase and several nonlamellar phases. The features of the glass transition in phospholipids are similar to other glass-forming materials, including plasticization by water and relaxation during annealing at sub- $T_g$  temperatures. The  $T_g$  appears to be relatively insensitive to the hydrocarbon chain length but is sensitive to the type of polar group and phase state. Combining the results of the current investigation of the PC species with the earlier observations of a  $T_g$  for PE,<sup>5,24</sup> it can be assumed that the presence of a glass transition is probably a common feature of most phospholipids and biological membranes.

Note that the majority of the  $T_g$  values were obtained for lipids in either the lamellar gel phase or in nonlamellar states, while there was a lack of any direct observation of a  $T_g$  in the lamellar liquid crystalline phase. A possible reason for the absence of a measurable  $T_g$  for the  $L_\alpha$  phase is that the  $L_\alpha$  is readily transformed to the gel phase upon cooling at relatively high temperatures, well above the expected  $T_g$ . This suggests that any comparison between the  $T_g$  in pure PC and possible  $T_g$  values in biological membranes should be made with caution. However, knowledge of the  $T_g$  for the gel phase can serve as a guide, since the  $T_g$  in the less ordered, liquid crystalline, phase can be expected to be lower than that of the more ordered gel phase. Moreover, knowing the  $T_g$  values of individual species would allow one to estimate the  $T_g$  in complex mixtures, e.g., biological membranes, using Gordon–Taylor or other appropriate equations allowing the calculation of the  $T_g$  of a mixture if the chemical composition and the  $T_g$  values of individual components are known.

**Acknowledgment.** This work was supported in part by a grant (DE-FG02-84ER13214) from the United States Department of Energy.

**Supporting Information Available:** Water content values obtained after equilibration of both liposomes and dried lipids at different RH conditions, as well as the temperatures of DSC thermal events; examples of DSC curves for both hydrated and dehydrated DOPC samples, as well as the transition temperatures. This material is available free of charge via the Internet at <http://pubs.acs.org>.

## References and Notes

- Quinn, P. J.; Wolf, C. *Biochim. Biophys. Acta, Biomembr.* **2009**, 1788, 33.
- Rappolt, M.; Laggner, P.; Pabst, G. *Recent Res. Dev. Biophys.* **2004**, 3 (2), 363.
- Steponkus, P. L.; Uemura, M.; Webb, M. S. *Permeability Stab. Lipid Bilayers* **1995**, 77.
- Nimtz, G.; Enders, A.; Binggeli, B. *Ber. Bunsen-Ges. Phys. Chem.* **1985**, 89, 842.
- Shalaev, E.; Steponkus, P. L. *J. Phys. Chem. B* **2003**, 107, 8734.
- Angell, C. A. *Chem. Rev.* **2002**, 102, 2627.
- Ediger, M. D.; Angell, C. A.; Nagel, S. R. *J. Phys. Chem.* **1996**, 100, 13200.
- Wunderlich, B. *Thermochim. Acta* **1999**, 37–52, 340.
- Hancock, B. C.; Zografi, G. *Pharm. Res.* **1994**, 11, 471.
- Saleki-Gerhardt, A.; Zografi, G. *Pharm. Res.* **1994**, 11, 1166.



- (11) Craig, I. D.; Parker, R.; Rigby, N. M.; Cairns, P.; Ring, S. G. *J. Agric. Food Chem.* **2001**, *49*, 4706.
- (12) Hill, J. J.; Shalaev, E. Y.; Zografi, G. *J. Pharm. Sci.* **2005**, *94*, 1636.
- (13) Diomaev, A. K.; Lanyi, J. K. *Biochemistry* **2008**, *47*, 11125.
- (14) (a) Franks, F. *Pure Appl. Chem.* **1997**, *69*, 915. (b) Slade, L.; Levin, H. *Crit. Rev. Food Sci. Nutrition* **1991**, *30*, 115.
- (15) Burke, M. J. In *Membranes, Metabolism, and Dehydrated Organisms*; Leopold, A. C., Ed.; Cornell University Press: Ithaca, NY, 1986; pp 358–363.
- (16) Zhang, J.; Steponkus, P. L. *Cryobiology* **1996**, *33*, 624.
- (17) Koster, K. L.; Webb, M. S.; Bryant, G.; Lynch, D. V. *Biochim. Biophys. Acta* **1994**, *1193*, 143.
- (18) Wolfe, J.; Bryant, G. *Cryobiology* **1999**, *39*, 103.
- (19) Blöcher, D.; Gutermann, R.; Henkel, B.; Ring, K. *Biochim. Biophys. Acta* **1984**, *778*, 74.
- (20) Blöcher, D.; Six, L.; Gutermann, R.; Henkel, B.; Ring, K. *Biochim. Biophys. Acta* **1985**, *818*, 333.
- (21) Fitter, J.; Lechner, R. E.; Dencher, N. A. *J. Phys. Chem.* **1999**, *103*, 8036.
- (22) Voinova, M. V. *Thermochim. Acta* **1996**, *280/281*, 465.
- (23) Voinova, M. V. *Colloids Surf. A: Physicochem. Eng. Aspects* **1995**, *95*, 133.
- (24) Shalaev, E.; Steponkus, P. L. *Biochim. Biophys. Acta* **2001**, *1514*, 100.
- (25) Shalaev, E. Y.; Steponkus, P. L. *Thermochim. Acta* **2000**, *345*, 141.
- (26) Bergestahl, B.; Stenius, P. *J. Phys. Chem.* **1987**, *91*, 5944.
- (27) Shalaev, E. Y.; Steponkus, P. L. *Biochim. Biophys. Acta* **1999**, *1419*, 229.
- (28) Janiak, M. J.; Small, D. M.; Shipley, G. G. *J. Biol. Chem.* **1979**, *254*, 6068.
- (29) Levine, H.; Slade, L. In *Water Science Reviews*; Franks, F., Ed.; Cambridge University Press: Cambridge, UK, 1988; Vol. 3, p 79.
- (30) (a) Angell, C. A. *Science* **1995**, *267*, 1924. (b) Shamblyn, S. L.; Hancock, B. C.; Zografi, G. *Eur. J. Pharm. Biopharm.* **1998**, *45*, 239.
- (31) Gordon, M.; Taylor, J. S. *J. Appl. Chem.* **1952**, *2*, 493.
- (32) Sugisaki, M.; Suga, H.; Seki, S. *Bull. Chem. Soc. Jpn.* **1968**, *41*, 2591.
- (33) Hancock, B. C.; Zografi, G. *Pharm. Res.* **1994**, *11*, 471. Note that  $k$  values reported in ref 33 are related to  $K$  values in the present paper as  $K = 1/k$ .
- (34) Bellavia, G.; Cottone, G.; Giuffrida, S.; Cupane, A.; Cordone, L. *J. Phys. Chem. B* **2009**, *113*, 11543.
- (35) (a) Contard, N.; Ring, S. *J. Agric. Food Chem.* **1996**, *44*, 3474. (b) Orford, P. D.; Parker, R.; Ring, S. G.; Smith, A. C. *Int. J. Biol. Macromol.* **1989**, *11*, 91. (c) Kalichevsky, M.; Blanshard, J.; Tokarczuk, P. *Int. J. Food Technol.* **1993**, *28*, 1390. (d) Kalichevsky, M.; Jaroszkiewicz, E. M.; Blanshard, J. M. V. *Int. J. Biol. Macromol.* **1992**, *14*, 257.
- (36) Crowley, K. J.; Zografi, G. *Thermochim. Acta* **2001**, *380*, 79.
- (37) Mansour, H. M.; Zografi, G. *J. Pharm. Sci.* **2007**, *96*, 377.
- (38) Svanberg, C.; Berntsen, P.; Johansson, A.; Hedlung, T.; Axen, E.; Swenson, J. *J. Chem. Phys.* **2009**, *130*, 035101.
- (39) Dozastakis, M.; Garcia Sakai, V.; Ohtake, S.; Maranas, J. K.; de Pablo, J. J. *Biophys. J.* **2007**, *92*, 147.
- (40) Castellano, C.; Generosi, J.; Congiu, A.; Cantelli, R. *Appl. Phys. Lett.* **2006**, *89*, 233905.
- (41) Dzuba, S. A.; Watari, H.; Shimoyama, Y.; Maryasov, A. G.; Kadera, Y.; Kawamori, A. *J. Magn. Reson. A* **1995**, *115*, 80.
- (42) Ngai, K. L. *J. Non-Cryst. Solids* **1996**, *197*, 1.
- (43) Hsieh, C.-H.; Wu, W.-G. *Biophys. J.* **1996**, *71*, 3278.
- (44) (a) Hsieh, C. H.; Wu, W. *Chem. Phys. Lipids* **1995**, *78*, 37. (b) Wu, W.; Chi, L.-M.; Yang, T.-S.; Fang, S.-Y. *J. Biol. Chem.* **1991**, *266*, 13602.
- (45) Surovtsev, N. V.; Dzuba, S. A. *J. Phys. Chem. B* **2009**, *113*, 15558.

JP910348Y